Published OnlineFirst December 18, 2014; DOI: 10.1158/1535-7163.MCT-14-0762

Molecular Cancer Therapeutics

Clinical and Cellular Roles for TDP1 and TOP1 in Modulating Colorectal Cancer Response to Irinotecan

Cornelia Meisenberg[1], Duncan C. Gilbert[2], Anthony Chalmers[3], Vikki Haley[4], Simon Gollins[5], Simon E. Ward[6], and Sherif F. El-Khamisy[1,7,8]

Abstract

Colorectal cancer is the third most common cancer in the world. Despite surgery, up to 50% of patients relapse with incurable disease. First-line chemotherapy uses the topoisomerase 1 (TOP1) poison irinotecan, which triggers cell death by trapping TOP1 on DNA. The removal of TOP1 peptide from TOP1–DNA breaks is conducted by tyrosyl-DNA phosphodiesterase 1 (TDP1). Despite putative roles for TDP1 and TOP1 in colorectal cancer, their role in cellular and clinical responses to TOP1-targeting therapies remains unclear. Here, we show varying expression levels of TOP1 and TDP1 polypeptides in multiple colorectal cancer cell lines and in clinical colorectal cancer samples. TDP1 overexpression or TOP1 depletion is protective. Conversely, TDP1 depletion increases DNA-strand breakage and hypersensitivity to irinotecan in a TOP1-dependent manner, presenting a potential therapeutic opportunity in colorectal cancer. TDP1 protein levels correlate well with mRNA and with TDP1 catalytic activity. However, no correlation is observed between inherent TDP1 or TOP1 levels alone and irinotecan sensitivity, pointing at their limited utility as predictive biomarkers in colorectal cancer. These findings establish TDP1 as a potential therapeutic target for the treatment of colorectal cancer and question the validity of TOP1 or TDP1 on their own as predictive biomarkers for irinotecan response. *Mol Cancer Ther; 14(2); 575–85. ©2014 AACR.*

Introduction

Colorectal cancer remains one of the most significant malignancies to affect populations with 39,000 new cases per year and 16,000 deaths in the United Kingdom and 177,000 new cases per year and 58,000 deaths in the United States (1). Although surgical excision of localized tumors is the primary treatment modality, up to 50% of patients subsequently experience relapse and many more present with metastatic disease at the outset. Standard first-line chemotherapy entails a combination of folinic acid, 5-fluorouracil, and either irinotecan (FOLFIRI) or oxaliplatin (FOLFOX), for which there is broad equivalence in tumor response (2). Interestingly, irinotecan and oxaliplatin do not seem to generate common resistance mechanisms and the alternate combination is commonly used as second-line therapy. Given the broad equivalence of efficacy in the first- and second-line settings between oxaliplatin and irinotecan, biomarkers predicting differential response would play a significant role in optimizing treatment protocols.

Irinotecan (CPT-11) is a prodrug that is converted within the cell to its active metabolite SN38, a potent camptothecin-based topoisomerase 1 (TOP1) poison. Its efficacy in treating metastatic colorectal cancer was first demonstrated over a decade ago in clinical trials with response rates of 50% and improved overall survival approaching 24 months (3, 4). Although forming a standard of care in the management of metastatic colorectal cancer, a role for irinotecan is also being investigated in the neoadjuvant treatment of locally advanced rectal cancer (5–7) where it is the subject of the ongoing ARISTOTLE trial (http://www.controlled-trials.com/ISRCTN09351447). The continuing inclusion of irinotecan in clinical trial protocols highlights the urgency and importance of identifying biomarkers for tumor response and novel means by which to improve irinotecan efficacy in the clinic. Both TOP1 and aprataxin levels have been shown to correlate with irinotecan sensitivity in colorectal cancer and PARP-1 inhibition may furthermore potentiate irinotecan sensitivity in the clinic (8–11).

TOP1 is an important cellular enzyme that allows for DNA relaxation, thus facilitating the processes of transcription and replication. In this role, TOP1 cleaves DNA to create a DNA single-strand break (SSB) to which it remains covalently bound to, thus allowing for rotation and relaxation of DNA (12). Once rotated, bound TOP1 ligates the nicked DNA and is released. TOP1 poisons prevent TOP1 ligase activity and subsequent release, and therefore promote SSB persistence and DNA double-strand break (DSB) formation at replication forks, collectively

[1]The Wellcome Trust DNA Repair Group, Genome Damage and Stability Centre, University of Sussex, Brighton, United Kingdom. [2]Sussex Cancer Centre, Royal Sussex County Hospital, Brighton, United Kingdom. [3]Institute of Cancer Sciences, University of Glasgow, Glasgow, United Kingdom. [4]Faculty of Science, Department of Life, Health and Chemical Sciences, The Open University, Milton Keynes, United Kingdom. [5]North Wales Cancer Treatment Centre, Betsi Cadwaladr University of Health Board, Ysbty Glan Clwyd, Bodelwyddan, Rhyl, United Kingdom. [6]Translational Drug Discovery Group, School of Life Sciences, University of Sussex, Brighton, United Kingdom. [7]Mammalian Genome Stability Group, Krebs Institute, Department of Molecular Biology and Biotechnology, University of Sheffield, Sheffield, United Kingdom. [8]Center of Genomics, Helmy Institute, Zewail City of Science and Technology, Giza, Egypt.

Corresponding Author: Sherif F. El-Khamisy, University of Sheffield, Firth Court Sheffield, S10 2TN, United Kingdom. Phone: 44-79199-27744; Fax: 44-114-2222-791; E-mail: s.el-khamisy@sheffield.ac.uk

doi: 10.1158/1535-7163.MCT-14-0762

Published OnlineFirst December 18, 2014; DOI: 10.1158/1535-7163.MCT-14-0762

known as protein-linked DNA breaks (PDB; refs. 13–18). Unrepaired DSBs activate cell-cycle arrest and trigger apoptosis-mediated cell death. The effectiveness of TOP1 poisons in killing cancer cells is therefore thought to be primarily dependent on levels of TOP1 and the rate of repair of TOP1-mediated DNA damage.

Cellular removal of TOP1–DNA breaks involves proteasomal degradation of TOP1 to leave a small peptide linked to DNA via a 3′-phosphotyrosyl linkage that is removed by tyrosyl-DNA phosphodiesterase 1 (TDP1) before repair completion by the DNA SSB repair pathway (19–23). TDP1 is involved early on in the repair process and its activity is critical for repair (24–28). TDP1 is additionally able to process 3′-phosphoglycolate moieties that are induced by ionizing radiation (IR) and therefore plays a role in the resolution of DNA damage associated with both TOP1 poisoning and IR (29–32). TDP1 inhibition may therefore be particularly well suited to improving the efficacy of radiotherapy delivered in combination with TOP1 targeting chemotherapies. Indeed, multiple drug screening efforts to identify TDP1 inhibitors are currently under way (33–35).

In this study, we examined the role of TDP1 in determining colorectal cancer responses to irinotecan. We observed a broad range of TDP1 and TOP1 protein levels in both colorectal cancer cell lines and clinical colorectal cancer samples. TDP1 and TOP1 protein correlate well with their respective mRNA levels whereas TDP1 protein expression correlates well with its catalytic activity *in vitro*. TDP1 depletion increased DNA-strand breakage and hypersensitivity to irinotecan in a TOP1-dependent manner while TOP1 loss or TDP1 overexpression proved to be protective, presenting a potential therapeutic opportunity in colorectal cancer.

Materials and Methods

Cells

Human colorectal cancer cell lines were obtained from the ATCC, LGC Standards, Middlesex United Kingdom in 2013. The cell lines were tested and authenticated by the supplier and further tested in our laboratory using morphologic assessment, PCR-based methods, and DNA staining (Hoechst 33258; Sigma). Cells were confirmed to be *Mycoplasma* free before embarking the study, stored in multiple early passages, and cultured for a period not exceeding 5 months. Cells were maintained in a 5% CO_2 incubator at 37°C. SW480 and SW48 were grown in Leibovitz L-15 media (20% FCS and 2 mmol/L L-glutamine), DLD1 and LS174T were grown in DMEM (10% FCS and 2 mmol/L L-glutamine) whereas Caco2 was cultured in DMEM (20% FCS and 2 mmol/L L-glutamine) and RKO in RPMI (10% FCS and 2 mmol/L L-glutamine). All media were Gibco products obtained from Life Technologies.

Whole-cell extract preparation

Adhered cells were washed twice in ice-cold phosphate-buffered saline (PBS) and collected by scraping and centrifugation at 1,500 rpm for 5 minutes. Extraction was carried out using ice-cold lysis buffer (20 mmol/L Tris–HCl pH 7.5, 10 mmol/L EDTA pH 8.0, 100 mmol/L NaCl, and 1% Triton X-100) supplemented with Complete Mini EDTA-free Protease Inhibitor Cocktail (Roche Applied Science). Extraction was carried out on ice for 30 minutes, the lysate was cleared by centrifugation at 13,000 rpm for 10 minutes, and the supernatant was collected as whole-cell extract (WCE). Total protein concentration was determined by Bradford assay and the samples stored at −80°C.

Western blotting

WCE (40 μg) was separated by 10% SDS-PAGE at 125 V for 2 hours and transferred on to a Hybond-C Extra Nitrocellulose membrane (Fisher Scientific UK) at 25 V for 90 minutes. The membranes were blocked in 5% PBS–milk for 1 hour before overnight incubation with antibodies against TDP1 (ab4166; Abcam), TOP1 (SC-32736; Santa Cruz Biotechnology), and actin (A4700; Sigma-Aldrich) diluted in 5% PBST–milk at 1:2,000, 1:1,000, and 1:3,000, respectively. The membranes were washed three times in PBST and incubated for 1 hour in 5% PBST–milk containing either horseradish peroxidase (HRP)–labeled polyclonal rabbit anti-mouse or polyclonal goat anti-rabbit secondary antibodies (Dako) at a 1:3,000 dilution. The chemiluminescent detection reagent, SuperSignal West Pico Chemiluminescent Substrate (Fisher Scientific UK), was used for blot development and bands were quantified using the ImageJ software.

Quantitative PCR

Total mRNA was purified from cells using the RNeasy Kit (Qiagen) and mRNA concentration was measured using the NanoDrop 1000 spectrophotometer (NanoDrop) at OD of 230 nm. The SuperScript First-Strand RT-PCR System (Invitrogen) was used to generate cDNA from 1 μg of total mRNA. Real-time PCR analysis was carried out on the MX3005p qPCR system (Agilent Technologies) using Blue qPCR SYBR Low ROX Mix (Fisher Scientific) and primers targeting exon-crossing regions for TDP1 (forward, 5′-CCCCTTCCAGTTTTACCTCAC-3′; reverse, 5′-AGTCCACGTCAAAGCAGTAG-3′), TOP1 (forward, 5′-ACGAATCAAGGGTGAGAAGG-3′; reverse, 5′-CGATACTGGTTCCGGATCTT-3′), and GAPDH (forward, 5′-ACATCGCTCAGACACCATG-3′; reverse, 5′-TGTAGTTGAGGTCAATGAAGGG-3′) ordered from Eurogentec. Relative quantitation (RQ) of mRNA was calculated as $RQ = 2^{\Delta\Delta C_T}$, where C_T is the average cycle threshold for three readings.

TDP1 activity assay

In vitro 3′-tyrosyl-DNA phosphodiesterase activity was measured using a gel-based 3′-tyrosyl-DNA phosphodiesterase activity assay. Reactions (10-μL total) were carried out in assay buffer (25 mmol/L HEPES, pH 8.0, 130 mmol/L KCl, and 1 mmol/L dithiothreitol) containing 50 nmol/L 5′-Cy5.5-labeled substrate, 5′-(Cy5.5)GATCTAAAAGACT(pY)-3′ (The Midland Certified Reagent Company), and indicated amounts of WCE (ng) or recombinant human TDP1 protein described in ref. (25). The reactions progressed at 37°C for 1 hour and were quenched with 10 μL of loading buffer (44% deionized formamide, 2.25 mmol/L Tris–borate, 0.05 mmol/L EDTA, 0.01% xylene cyanol, and 1% bromophenol blue) before heating at 90°C for 10 minutes and separation on a 20% Urea SequaGel (Fisher Scientific) run at 190 V for 2 hours in 1 × TBE. Gels were imaged using the FujiFilm Fluor Imager FLA-5100 at 635 nm and bands were quantified using the ImageJ software.

Clonogenic survival assay

Colorectal cancer sensitivity to irinotecan (CPT-11) and irradiation (IR) was measured by clonogenic survival assay. Briefly, adhered cells seeded at dose-dependent densities (300–2,400 per 10-cm dish) were treated with gamma radiation (1–4 Gy using a ^{137}Cs γ-ray source at a rate of 1 Gy/9-s exposure) or with media containing CPT-11 (Sigma-Aldrich) or DMSO and incubated in a 5% CO_2 incubator at 37°C for 7 to 12 days to allow for colony formation (>50 cells). The colonies were fixed and stained using

Published OnlineFirst December 18, 2014; DOI: 10.1158/1535-7163.MCT-14-0762

0.4% methylene blue in 50% methanol before counting. The surviving fraction was calculated as the surviving colony fraction (colonies counted/total cells seeded) of the treatment plates divided by that of the untreated plates.

Plasmid transfection

Cells were transfected with the pCI-neo-Myc vector or that encoding human TDP1 using Lipofectamine LTX plus reagent (Invitrogen). Briefly, plasmid amounts (μg) were suspended in 200 μL of FCS-free media and mixed with 200 μL of FCS-free media containing 7.5 μL of LTX reagent and 3 μL of Plus reagent before a 5-minute incubation at room temperature. The mixture was added to 6-cm dishes containing 6×10^5 adhered cells in 3-mL FCS media and the cells were incubated at 37°C for 24 hours before harvesting for further use.

mRNA silencing

For mRNA silencing, 10 μL of Lipofectamine 2000 RNAiMAX reagent (Invitrogen) added to 250 μL FCS-free media was incubated at room temperature for 5 minutes and added to 250 μL of FCS-free media containing the indicated siRNA sequences. The mixture was incubated at room temperature for 20 minutes before adding to 6-cm dishes containing 3×10^5 cells in 3-mL FCS media. For TDP1 siRNA, cells were treated first in suspension and again 6 hours later. For combined TDP1/TOP1 siRNA treatment, TOP1 siRNA was carried out 16 hours after the second TDP1 siRNA treatment. The plates were incubated at 37°C for a total of 72 hours for TDP1 siRNA and 48 hours for TOP1 siRNA before harvesting for further use. Both TDP1 and TOP1 siRNA sequence pools were bought as Dharmacon ON-TARGET*plus* smartpools (Fisher Scientific) while the BLAST validated scrambled siRNA sequence (5′-UUCUUCGAACGUGUCACGU-3′) and individual TDP1 siRNA sequences (TDP1si-05: 5′-GGAGUUAAGCCAAAGUAUA-3′, TDP1si-06: 5′-UCAGUUACUUGAUGGCUUA-3′, TDP1si-07: 5′-GACCAUAUCUAGUAGUGAU-3′, and TDP1si-08: 5′-CUAGACAGUUUCAAAGUGA-3′) were obtained from Eurogentec.

Alkaline comet assay

DNA SSBs were measured by alkaline comet assay (ACA; ref. 36). Cells in suspension were treated with media containing DMSO or 50 μmol/L CPT-11 for 1 hour. The cells washed once in ice-cold PBS and mixed at 1:1 with 1.2% low-melt agarose before layering onto prechilled frosted glass slides precoated with 0.6% agarose. The slides were subsequently immersed in ice-cold lysis buffer (2.5 mol/L NaCl, 100 mmol/L EDTA pH 8.0, 10 mmol/L Tris–HCl, 1% Triton X-100, and 1% DMSO; pH 10) for 1 hour at 4°C followed by DNA unwinding in electrophoresis buffer (50 mmol/L NaOH, 1 mmol/L EDTA, and 1% DMSO) for 45 minutes before electrophoresis at 12 V for 25 minutes. The slides were neutralized overnight in 0.4 mol/L Tris–HCl (pH 7.0) and stained with SYBR-Green (1:10,000 in PBS) for 10 minutes. The tail moments for 100 cells per sample were scored using the Comet Assay IV software (Perceptive Instruments).

Immunostaining

Cell monolayers grown to subconfluent densities on coverslips were treated with media containing DMSO or 1 μmol/L CPT-11 for 1.5 hours. The cells were washed twice in warmed PBS and left to recover in fresh media for 2 hours. After washing twice in ice-cold PBS, the cells were fixed with 3.7% paraformaldehyde for 10 minutes at room temperature and permeabilized in 0.2% Triton-X in PBS for 3 minutes on ice. The coverslips were washed three times in PBS, blocked in 2% BSA-Fraction V for 30 minutes before incubation with γ-H2AX primary antibodies (JBW301; Millipore) diluted at 1:800 in 2% BSA-Fraction V for 45 minutes. The coverslips were washed three times in PBS and incubated with FITC-labeled secondary antibodies (Sigma-Aldrich) diluted at 1:300 in 2% BSA-Fraction V for 45 minutes. The coverslips were rinsed in PBS three times and mounted onto slides using Vectashield-containing DAPI (Vector Laboratories) before visualizing and scoring on a Nikon Eclipse e-400 microscope.

Immunohistochemistry

Tissue microarray (TMA) slides consisting of 59 formalin-fixed, paraffin-embedded colorectal cancer samples with documented tumor demographic and correlated overall survival data were obtained from Imgenex (IMH-306). These were deparaffinized and stained with antibodies for TDP1 (NB100-81642; Novus Biologicals) and TOP1 (NCL-TOPO1; Leica Microsystems), both at 1:200 dilution using a Bond Max Autostainer. Cores were classified as none, low, moderate, or high for TDP1 and TOP1 staining, with samples recorded if >5% cells stained accordingly. Rectal adenocarcinoma samples with known chemoradiotherapy response outcomes were obtained with appropriate consent from a cohort of patients treated on the RICE study (5). Specifically, these were from patients with locally advanced rectal adenocarcinomas treated with a neoadjuvant regimen of pelvic radiotherapy (45 Gy in 25 fractions over 5 weeks) with concurrent oral capecitabine (650 mg/m^2 twice daily, continuously days 1–35) and irinotecan (60 mg/m^2 intravenously once weekly, weeks 1–4) before surgical resection. These were similarly stained for TDP1 expression and classified as above.

Results

To examine the role of TDP1 in colorectal cancer, we first characterized the cellular variation of TDP1 and TOP1 protein levels in a panel of six colorectal cancer cell lines (RKO, SW480, SW48, Caco2, DLD1, and LS147T). WCE prepared from each of the six cell lines were analyzed by Western blotting using antibodies against TDP1, TOP1, and actin (Fig. 1A–C). Because actin is normally used as a loading control for the comparison of isogenic samples in a Western blot analysis and our panel consists of nonisogenic cell lines, we instead loaded equal amounts of extract (40 μg) and normalized TDP1 and TOP1 levels directly to that obtained for the highest expressor, the RKO cell line. Our results show varying levels of TDP1 and TOP1 expression within the colorectal cancer panel. For diagnostic and drug design purposes, it is important to understand the nature of such variation. We thus carried out qPCR to measure the levels of TDP1 and TOP1 mRNA. Purified total mRNA was reverse transcribed into cDNA that was further amplified using primers against exon-crossing regions for TDP1 and TOP1 cDNA. The cycle threshold obtained was used to quantify relative TDP1 and TOP1 mRNA levels normalized to that obtained for the RKO cell line (Fig. 1D and E). Pearson correlation coefficients for TDP1 protein and mRNA levels ($R = 0.884$; $P = 0.019$) and TOP1 protein and mRNA levels ($R = 0.870$; $P = 0.024$) were significantly positive (Fig. 1F and G). We conclude from these experiments that TDP1 and TOP1 display remarkable variation in colorectal cancer cell lines and that protein expression correlates well with corresponding levels of mRNA.

Published OnlineFirst December 18, 2014; DOI: 10.1158/1535-7163.MCT-14-0762

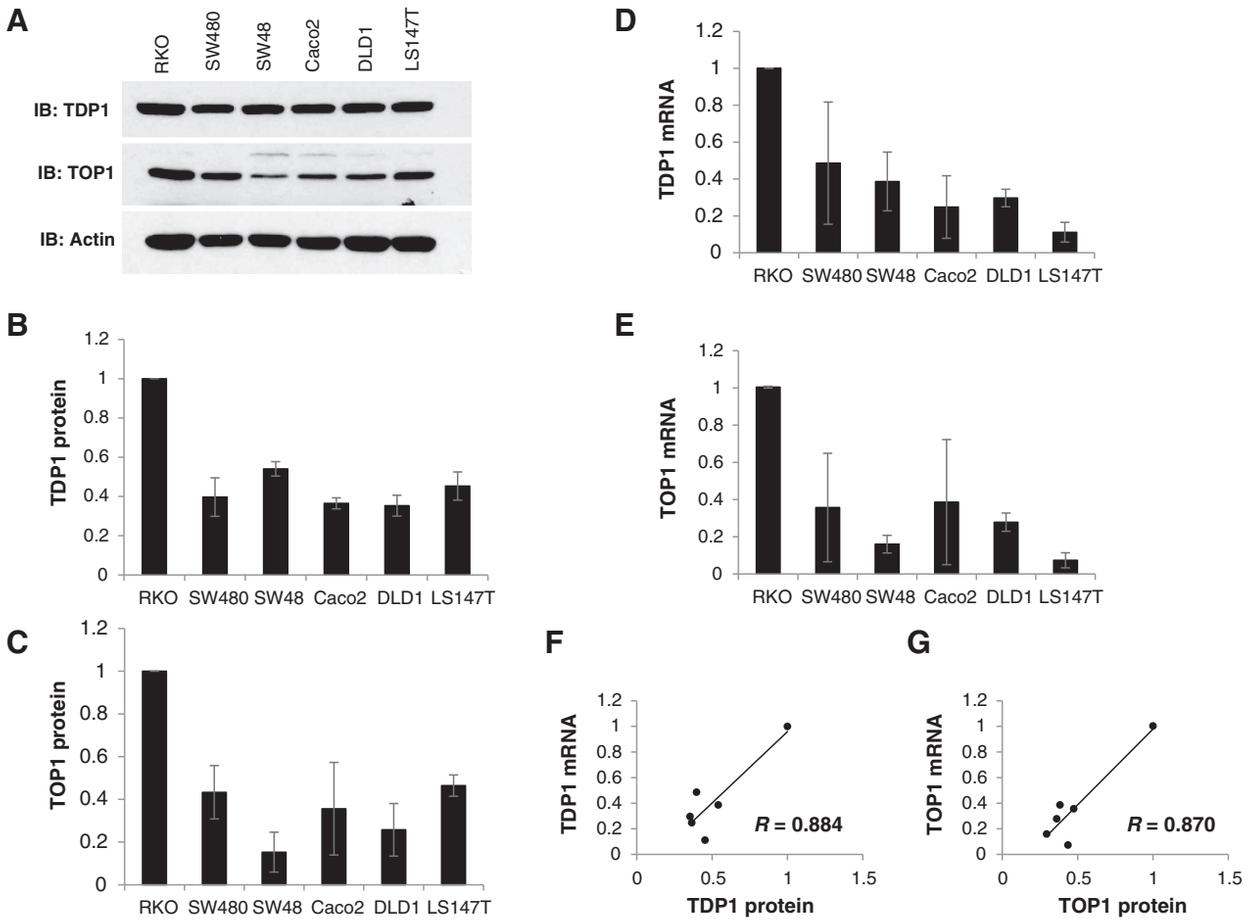

Figure 1.
TDP1 and TOP1 protein levels correlate positively with TDP1 and TOP1 mRNA levels in colorectal cancer cell lines. A, colorectal cancer WCE (40 μg) was separated by 10% SDS–PAGE and analyzed by Western blotting using antibodies against TDP1, TOP1, and actin. The bands were quantified using the ImageJ software and relative TDP1 (B) and TOP1 (C) protein levels normalized to that obtained for RKO are shown ± STD for three independent experiments. mRNA (1 μg) purified from the colorectal cancer cell lines was reverse transcribed into cDNA that was used for real-time PCR analysis using primers against exon-crossing regions for TDP1 and TOP1. The relative quantity of mRNA (RQ value) for TDP1 (D) and TOP1 (E) was calculated as RQ = $2^{-\Delta\Delta C_T}$ and normalized to that obtained for the RKO cell line; the average from three independent experiments ± STD is depicted. A graphical representation of the Pearson correlation coefficient (*R*) between colorectal cancer TDP1 protein and mRNA levels is shown in F and for TOP1 protein and mRNA levels in G.

To gain further insight into the extent of TDP1 and TOP1 variation in colorectal cancer, we used a commercially available TMA containing 59 colorectal cancer samples to assess TDP1 and TOP1 protein levels. Within normal colonic epithelium, TDP1 staining was seen to be primarily nuclear, in both epithelial and crypt cells (Fig. 2A). The 59 colorectal cancer samples demonstrated a range of protein expression for both TDP1 and TOP1 (Fig. 2B and C) with the majority showing moderate to strong staining for both TDP1 (69%) and TOP1 (77%). Although there was no significant overall correlation between TDP1 and TOP1 protein levels ($R = 0.24$; $P = 0.075$), it was noted that of the 42 samples that scored moderate/high for TOP1, 72% showed moderate to high TDP1 staining. Interestingly, there appears to be no difference in staining frequencies between tumors selected from different anatomic sites (Table 1). We also carried out TDP1 immunohistochemistry (IHC) on 125 rectal cancer specimens acquired from the RICE trial of neoadjuvant irinotecan, capecitabine, and radiotherapy treatment (Fig. 2D and E; ref. 5). Although a variation in TDP1 was again identified, overall these specimens exhibited lower expression of TDP1 than those in the TMA samples. We conclude from these observations that TDP1 and TOP1 expression also varies considerably in clinical colorectal cancer samples.

TDP1 is a key "bottleneck" repair factor for damage caused by TOP1 targeting therapies and is therefore regarded as a promising therapeutic target for inhibition (32, 37). Our findings that colorectal cancer possesses varying levels of TDP1 prompted us to test whether TDP1 plays a role in colorectal cancer responses to irinotecan. We initially depleted TDP1, TOP1, or both from RKO and SW480 cell lines using siRNA-targeting sequence pools (4 sequences per pool). Cells were subsequently subjected to clonogenic survival assay to measure cell sensitivity to CPT-11 (Fig. 3A and D) or irradiation (Fig. 3B and E), and for Western blot analysis using antibodies against TDP1, TOP1, and actin (Fig. 3C and F). We established conditions that led to >80% depletion of both endogenous TDP1 and TOP1 on their own and in combination. Using a gel-based TDP1 activity assay, we furthermore confirmed that TDP1 siRNA-treated RKO cells possess only 10% of their 3′-tyrosyl-DNA phosphodiesterase activity compared with

Published OnlineFirst December 18, 2014; DOI: 10.1158/1535-7163.MCT-14-0762

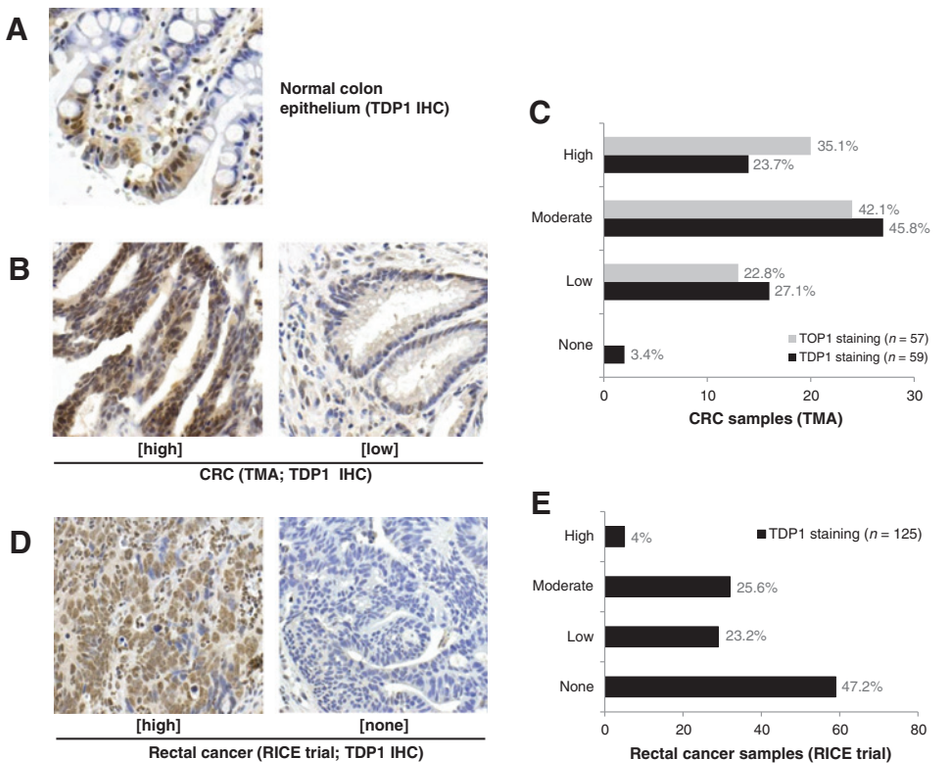

Figure 2.
TDP1 and TOP1 protein levels vary widely in colorectal cancer (CRC) patient samples. A, a representative IHC image for TDP1 (NB100-81642; Novus Biologicals) in normal colon epithelium showing nuclear staining in crypt and in surface epithelium cells. B, representative IHC images for high and low TDP1 staining in colorectal cancer samples from a colorectal cancer TMA. C, distribution of staining intensity for TDP1 and TOP1 (NCL-TOPO1; Leica Microsystems) IHC on colorectal cancer samples from a TMA. D, representative IHC images for high and no TDP1 staining for rectal cancers obtained from the RICE trial. E, distribution of staining intensity for TDP1 IHC on rectal cancer samples obtained from the RICE trial.

scramble siRNA-treated RKO cells (Fig. 3G and H). The survival assay data show that for both cell lines, TDP1 siRNA-treated cells were significantly more sensitive to CPT-11 compared with scrambled siRNA-treated cells whereas the opposite was true for TOP1-depleted cells. Notably, these data further demonstrate that TDP1 depletion no longer sensitizes cells to CPT-11 if TOP1 is additionally depleted. TDP1-depleted RKO cells also demonstrated a slight increase in sensitivity to irradiation while this difference was more pronounced in SW480 cells. To rule out the possibility of off-target effects, we additionally show that depletion of TDP1 using four separate TDP1-targeting siRNA sequences also results in increased sensitivity of RKO cells to CPT-11 (Fig. 3I and J). We further show that TDP1-depleted RKO cells accumulate more DNA SSBs in the presence of CPT-11 as measured by ACA (Fig. 3K) and possess elevated levels of cytotoxic DNA DSBs as shown by immunostaining with γ-H2AX (Fig. 3L), compared with mock-treated counterparts. Together, we conclude that TDP1 depletion sensitizes colorectal cancer cells to irinotecan treatment in a TOP1-dependent manner and that TDP1 inhibition may further sensitize colorectal cancer to radiation therapy.

Table 1. TDP1 and TOP1 staining in tumors selected from different colorectal anatomic sites

	TDP1 staining			
	None	Low	Medium	High
Ascending	1	4	8	3
Cecum	0	2	1	0
Descending	0	1	3	1
Rectum	0	3	2	2
Sigmoid	1	4	9	7
Transverse	0	2	4	1

	TOP1 staining			
	None	Low	Medium	High
Ascending	0	4	8	4
Cecum	0	2	1	0
Descending	0	1	2	1
Rectum	0	0	3	3
Sigmoid	0	4	7	10
Transverse	0	2	3	2

NOTE: TMA slides of paraffin-embedded colorectal cancer samples with documented tumor demographic and correlated overall survival data were deparaffinized and stained with antibodies for TDP1 (NB100-81642; Novus Biologicals) and TOP1 (NCL-TOPO1; Leica Microsystems), both at 1:200 dilution using a Bond Max Autostainer. Scores were classified as none, low, moderate, or high for TDP1 and TOP1 staining, with samples recorded if >5% cells stained accordingly.

We next set out to test whether TDP1 overexpression would protect colorectal cancer cells from CPT-11–mediated cell death. Three colorectal cancer cell lines, RKO, SW480, and DLD1, were transfected with equimolar amounts of pCI-neo-myc plasmid that was either empty or encoding human TDP1. A clonogenic survival assay was carried out during which cells were treated with CPT-11 for the duration of colony formation (Fig. 4A, C, and E). The results showed that while TDP1 overexpression is protective in RKO and SW480 cell lines, the level of protection did not reach statistical significance in the less sensitive DLD1 cell line. Western blot analysis confirmed TDP1 overexpression in all cell lines (Fig. 4B, D, and F), which was further illustrated by a greater TDP1 catalytic activity in TDP1-transfected cells compared with control cells, for all three cell lines tested (Fig. 4G and H). Next, we examined whether the difference in CPT-11 survival is due to the ability of TDP1 to tolerate CPT-11–induced DNA-strand breakage. Our data demonstrate that RKO cells overexpressing TDP1 accumulate less DNA SSBs (Fig. 4I) and less DNA DSBs (Fig. 4J) than controls, as measured by ACA and γ-H2AX foci formation, respectively. We conclude that TDP1 overexpression protects

Published OnlineFirst December 18, 2014; DOI: 10.1158/1535-7163.MCT-14-0762

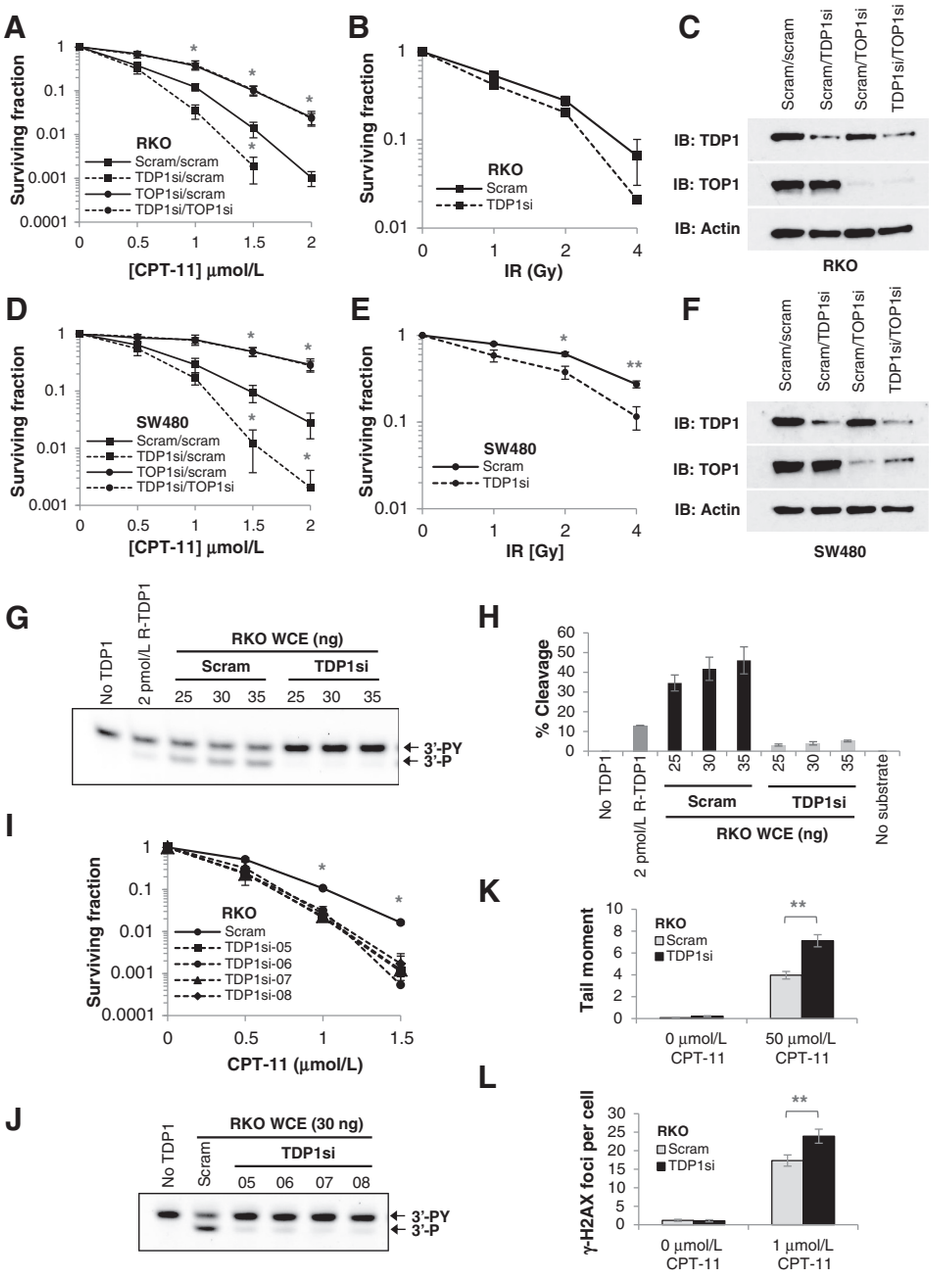

Figure 3.

TDP1 depletion sensitizes colorectal cancer cell lines to irradiation and to irinotecan treatment in a TOP1-dependent manner. RKO and SW480 cells transfected with nontargeting scrambled siRNA (Scram), a TDP1 siRNA pool (4 sequences) and/or a TOP1 siRNA pool (4 sequences) for 72 hours were subjected to a clonogenic survival assay during which they were continuously treated with CPT-11 for the duration of colony formation (7–12 days). The colonies were fixed, stained, and counted and the surviving fraction calculated and depicted as an average of three independent experiments ± SEM for RKO (A) and SW480 (D). TDP1 siRNA-treated RKO cells (B) and SW480 cells (E) were subjected to a survival assay for irradiation sensitivity and average surviving fraction of three independent experiments ± STD is shown. WCE (40 μg) generated from the siRNA-treated RKO (C) and SW480 (F) cells was analyzed further by 10% SDS-PAGE and Western blotting using antibodies against TDP1, TOP1, and actin. G, recombinant human TDP1 (2 pmol/L) and WCE (25, 30, and 35 ng) generated from either mock (Scram) or TDP1 siRNA-treated RKO cells were subjected to an *in vitro* TDP1 activity assay and the reaction products separated on a 20% Urea SequaGel before imaging at 635 nm. The substrate (3′-PY) and product (3′-P) are indicated by arrows. The bands were quantified using the ImageJ software and the average percentage of cleavage for three independent experiments ± STD is shown in H. TDP1 depletion was carried out in the RKO cell line using four separate TDP1 siRNA sequences (05 to 08). Cells were subsequently used in a clonogenic CPT-11 survival assay (I) or a gel-based TDP1 activity assay to measure knockdown efficiency (J). The average surviving fraction for two independent experiments ± STD is shown in I. K, TDP1 siRNA- or mock (scram)-treated RKO cells were treated with media containing either DMSO or 50 μmol/L CPT-11 for 1 hour and then subjected to analysis by ACA. The data shown are a representative single experiment ± STD for 100 cells per sample. L, TDP1 siRNA- or mock (scram)-treated RKO cells on coverslips were treated with media containing DMSO or 1 μmol/L CPT-11 for 1.5 hours and left to recover for 2 hours before fixing, permeabilizing, and staining with a γ-H2AX and a FITC-labeled secondary antibody. γ-H2AX foci were visualized and analyzed for 36 cells per sample on a Nikon Eclipse e-400 microscope. The average number of γ-H2AX foci per cell for three independent experiments is shown ± STD. A paired Student *t* test (two-tailed) statistical analysis shown as: *, $P < 0.05$; **, $P < 0.01$.

Published OnlineFirst December 18, 2014; DOI: 10.1158/1535-7163.MCT-14-0762

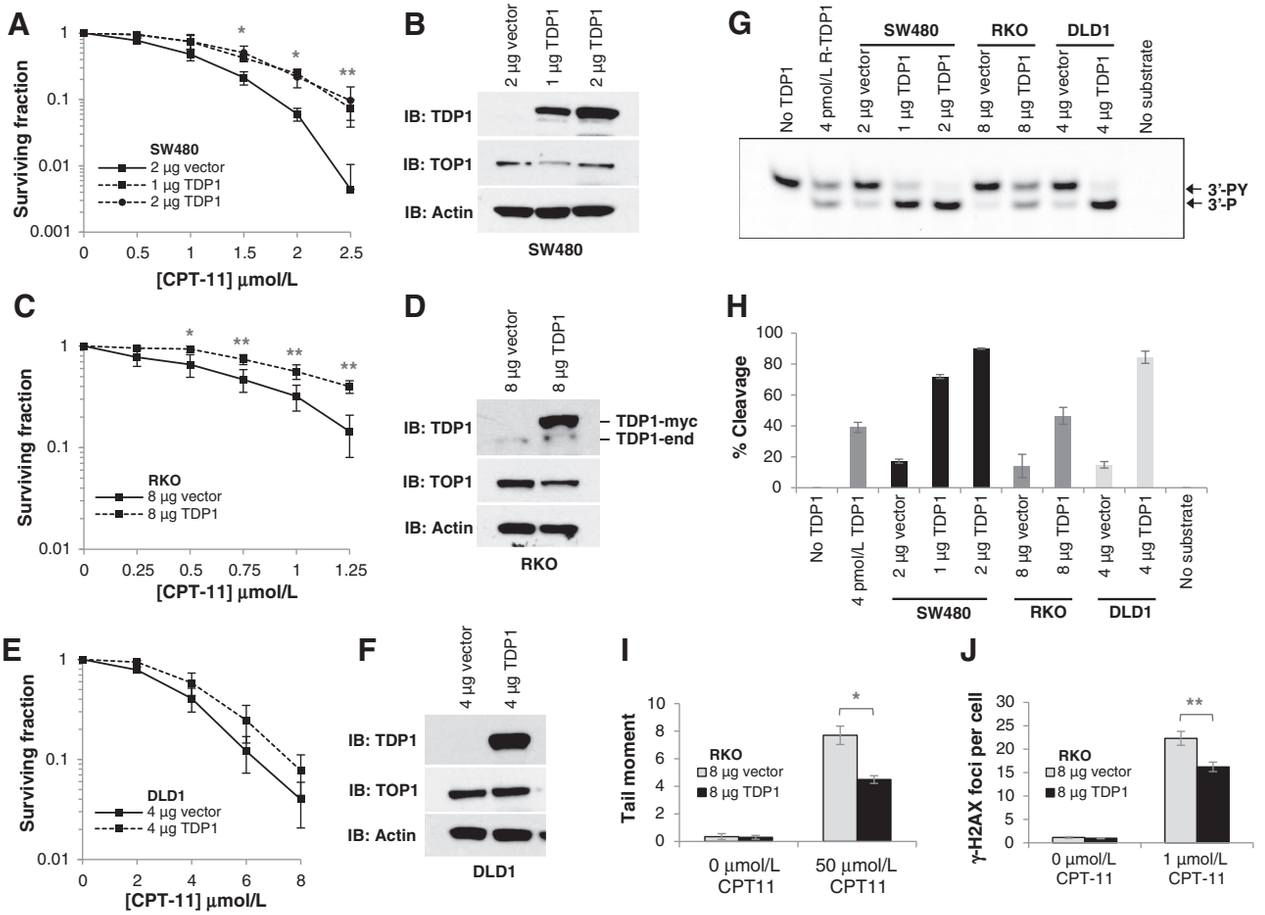

Figure 4.

TDP1 overexpression protects irinotecan-responsive colorectal cancer cells from irinotecan-mediated cell death. Colorectal cancer cell lines transfected with the indicated amounts of pCI-neo-myc vector or with pCI-neo-myc vector encoding human TDP1 were subjected to a clonogenic survival assay during which they were continuously treated with CPT-11 for the duration of colony formation (7–12 days). The colonies were fixed, stained, and counted and the surviving fraction calculated and depicted as an average of three independent experiments ± STD for the colorectal cancer cell lines SW480 (A), RKO (C), and DLD1 (E). WCE (40 μg) generated from the SW480 (B), RKO (D), and DLD1 (F) cell lines overexpressing either pCI-neo-myc vector or that encoding human TDP1 was analyzed by 10% SDS–PAGE and Western blotting using antibodies against TDP1, TOP1, and actin. The bands relating to overexpressed Myc-tagged TDP1 (TDP1-myc) and endogenous TDP1 (TDP1-end) are indicated. G, TDP1 activity assay reactions containing Cy5.5-labeled substrate and WCE for SW480 (25 ng), RKO (10 ng), and DLD1 (25 ng) overexpressing indicated amounts of pCI-neo-myc vector or that encoding human TDP1 were separated on a 20% Urea SequaGel and imaged at 635 nm. A recombinant human TDP1 (4 pmol/L) control was included. The substrate (3′-PY) and product (3′-P) are indicated by arrows. The bands were quantified using the ImageJ software and the average percentage of cleavage for three independent experiments ± STD is shown in H. I, RKO cells containing pCI-neo-myc empty vector or that encoding human TDP1 were treated with either DMSO or 50 μmol/L CPT-11 for 1 hour before analysis by ACA. Data shown are of three independent repeats ± STD. J, RKO cells overexpressing pCI-neo-myc vector or that encoding human TDP1 plated on coverslips were treated with DMSO or 1 μmol/L CPT-11 for 1.5 hours and left to recover for 2 hours before fixing, permeabilizing, and staining with a γ-H2AX and a FITC-labeled secondary antibodies. γ-H2AX foci were visualized and analyzed on a Nikon Eclipse e-400 microscope. The average number of γ-H2AX foci per cell for three independent experiments is shown ± STD. A paired Student *t* test (two-tailed) statistical analysis is shown as: *, $P < 0.05$; **, $P < 0.01$.

irinotecan-responsive colorectal cancer cells from irinotecan-mediated cytotoxicity.

The experiments outlined above suggest the potential of assessing TDP1 status as a useful clinical diagnostic tool to characterize patient samples. It is, however, essential to establish whether TDP1 protein levels correlate with its cellular activity. To test this, we measured TDP1 activity in colorectal cancer WCE using a 5′-Cy5.5-labeled oligonucleotide substrate containing a 3′-phosphotyrosine modification that is processed by TDP1 into an oligonucleotide product containing a 3′-phosphate group (Fig. 5A). WCE prepared from each of the six colorectal cancer cell lines were subjected to this assay and reaction products separated by 20% denaturing PAGE before gel imaging (Fig. 5B) and band quantification (Fig. 5C). We observed a variation in TDP1 activity that correlates significantly with TDP1 protein level ($R = 0.937$; $P = 0.006$ for 30-ng WCE and $R = 0.895$; $P = 0.016$ for 60-ng WCE; Fig. 5D and E). These observations suggest that measuring TDP1 protein level as a readout of its catalytic activity is suitable for the design of future clinical diagnostic tools.

A key clinical challenge facing the use of irinotecan is the lack of response in some patients. Therefore, we set out to test whether TDP1 levels could be used as a diagnostic marker for irinotecan response. To relate TDP1 and TOP1 protein levels to irinotecan response, we measured the inherent CPT-11 sensitivity of the

Published OnlineFirst December 18, 2014; DOI: 10.1158/1535-7163.MCT-14-0762

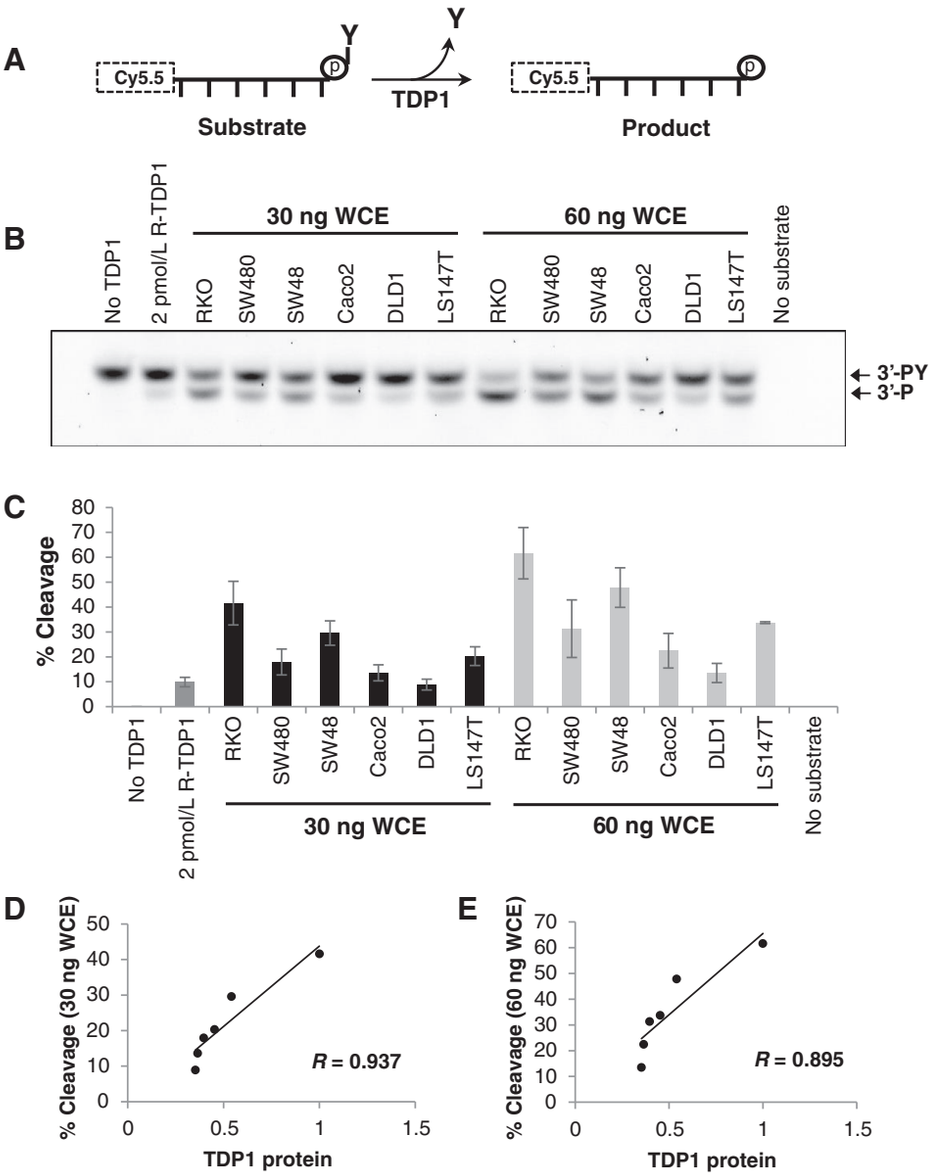

Figure 5.
In vitro TDP1 catalytic activity correlates positively with TDP1 protein levels in colorectal cancer cell lines. A, diagram depicting TDP1 processing of a 5′-Cy5.5-labeled oligonucleotide substrate harboring a 3′-phosphotyrosine modification (3′-PY) to form a Cy5.5-labeled oligonucleotide product harboring a 3′-phosphate (3′-P) that is smaller in size. B, 10-μL reaction volumes containing Cy5.5-labeled substrate and the indicated amounts of recombinant human TDP1 (2 pmol/L) or colorectal cancer WCE (ng) were separated on a 20% Urea SequaGel and imaged at 635 nm. The substrate (3′-PY) and product (3′-P) are indicated by arrows. C, reaction products were quantified using the ImageJ software and the average percentage of cleavage for three independent experiments ± STD is shown. A graphical representation of the Pearson correlation coefficient (*R*) between colorectal cancer TDP1 protein levels and percentage of cleavage for 30 ng WCE (D) or 60 ng WCE (E).

colorectal cancer cell lines using a clonogenic survival assay. Cells were treated continuously with CPT-11 for the duration of colony formation before fixing, staining, and counting. The results showed a significant variation in CPT-11 sensitivity between the six colorectal cancer cell lines, the least sensitive of which was DLD1 and the most sensitive was LS417T (Fig. 6A). However, subsequent analyses showed weak or lack of correlation between CPT-11 surviving fraction at 0.5 μmol/L CPT-11 (Fig. 6B) or 1.0 μmol/L CPT-11 (Fig. 6C) and TDP1 protein levels ($R = -0.377$, $P = 0.461$ and $R = -0.504$, $P = 0.308$, respectively) or TOP1 protein levels ($R = -0.169$, $P = 0.749$ and $R = -0.284$, $P = 0.585$, respectively). Because TDP1 repairs TOP1-mediated DNA damage, we normalized TDP1 levels to that of TOP1 but yet again found no significant correlation with sensitivity at 0.5 μmol/L CPT-11 ($n = 6$, two-tailed: $R = -0.270$, $P = 0.605$) or 1.0 μmol/L CPT-11 ($R = -0.278$; $P = 0.594$; Fig. 6B and C, right). For this latter analyses, removal of an apparent outlier cell line (SW48) highlighted a positive correlation, as would be expected if TDP1 and TOP1 were dominant determinants for irinotecan sensitivity (Fig. 6B and C, dotted line; $n = 5$, two-tailed: $R = 0.688$, $P = 0.199$ and $R = 0.773$, $P = 0.125$). These observations suggest that TDP1 and TOP1 protein levels alone do not correlate with irinotecan sensitivity in colorectal cancer cell lines, and that TDP1:TOP1 ratio may serve as a promising biomarker for irinotecan response.

To test whether this is also true in a clinical setting, we examined 125 rectal cancer samples acquired from the RICE trial for irinotecan/radiotherapy response. Criteria for irinotecan/radiotherapy responsiveness were pathologic complete remission (pCR) or microfoci of residual tumor (micR) only in the posttreatment (i.e., definitive surgical resection) specimen. Chemo/radiotherapy response was comparable between tumors with none/low TDP1 levels (35% pCR/micR positive) and those with moderate/high levels of TDP1 (39% pCR/micR positive; Fig. 6D), highlighting a lack of correlation between TDP1 level on its own and rectal

Published OnlineFirst December 18, 2014; DOI: 10.1158/1535-7163.MCT-14-0762

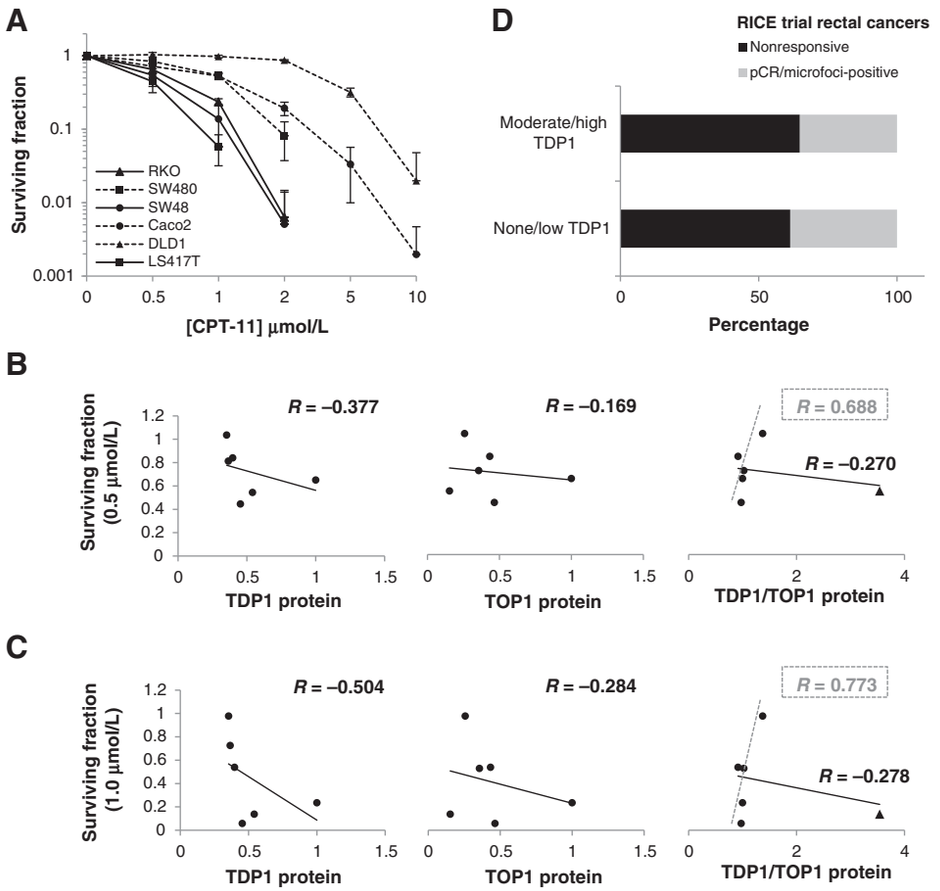

Figure 6.
TDP1 and TOP1 protein levels do not correlate with colorectal cancer irinotecan sensitivity. A, adhered colorectal cancer cells seeded on 10-cm dishes were subjected to CPT-11 treatment for the duration of colony formation (7–12 days). Colonies were fixed, stained, and counted and the surviving fraction calculated and depicted as an average of three independent experiments ± STD for each cell line. The Pearson correlation coefficient (*R*) between colorectal cancer surviving fraction at 0.5 μmol/L (B) or 1.0 μmol/L (C) CPT-11 treatment and TDP1 protein levels, TOP1 protein levels and TDP1:TOP1 protein level ratio is shown. For the latter, a correlation lacking data for SW48 cell lines (triangle) was also carried out (gray dotted line). D, irinotecan/radiotherapy response for rectal cancers obtained from the RICE trial was measured as nonresponsive or responsive if pCR or residual tumor (microfoci-positive) was observed and the distribution of response for none/low TDP1 rectal cancers or moderate/high TDP1 rectal cancers is shown.

cancer response to irinotecan/capecitabine/radiotherapy treatment. Of the 59 colorectal cancer cases on the TMA, with a mean follow-up of 122 months, 23 of 59 (39%) patients had died, 11 of which confirmed cancer. Neither TDP1 nor TOP1 expression was prognostic for overall survival (log-rank test, $P = 0.451$ for TDP1 and $P = 0.241$ for TOP1) or cancer-specific survival in these 59 patients (noting that numbers of events were small), although specific treatment details were unavailable. Together, these data challenge the utility of TDP1 or TOP1 alone as biomarkers for predicting the response of colorectal cancer to irinotecan but establish TDP1 as a potential therapeutic target in colorectal cancer.

Discussion

The TOP1 poison irinotecan has a major role in the chemotherapeutic management of advanced colorectal cancer. However, its use in the clinic is limited because some patients do not respond while others develop resistance. This study is aimed to gain an insight into the role of the key DNA repair enzyme TDP1 and irinotecan sensitivity in colorectal cancer. Our findings demonstrate that both TDP1 and TOP1 expression levels vary in a panel of colorectal cancer cell lines and in patient colorectal cancer samples as measured by IHC. We show that the majority of colorectal cancer samples assessed for TOP1 possessed either moderate or high levels. This is consistent with published data that suggest that colorectal cancer, especially rectal cancers, possess high levels of TOP1 (9, 38). In contrast to TOP1, no data are currently available on the expression and distribution of TDP1 in colorectal cancer. Here, we report that most colorectal cancer samples in the commercially available TMA possessed moderate to high levels of TDP1, whereas a larger proportion of the RICE trial samples of locally advanced rectal cancers expressed little or no TDP1. Whether this variation results from differences in sample preparation (e.g., whole section as opposed to TMA) or reflects true biological differences between tumor sites and stage is not clear. Future work characterizing additional clinical sample sets will aim to address this question and also how TDP1 expression might vary within individual tumors (intratumoral heterogeneity) and how this might change with time as the tumors are exposed to different treatments.

Unlike TOP1, the role for TDP1 in colorectal cancer cellular response to irinotecan has not been examined previously. We first addressed this putative role using TDP1 modulation studies, which revealed that TDP1 could influence significant changes in colorectal cancer response to irinotecan and to a lesser extent, irradiation. Our findings demonstrate that TDP1 overexpression protects colorectal cancer cells from CPT-11–mediated cell death. Conversely, TDP1 depletion sensitizes colorectal cancer cells to irinotecan, an effect that was mitigated by the additional depletion of TOP1. Together, these findings suggest that colorectal cancers may benefit from irinotecan and TDP1 inhibitor combination therapy in the clinic. It is, however, important that patient tumors are characterized for both TDP1 and TOP1 because TDP1 inhibition is unlikely to have an effect if TOP1 is not present or attenuated. To this end,

Published OnlineFirst December 18, 2014; DOI: 10.1158/1535-7163.MCT-14-0762

our colorectal cancer cell line data show that TDP1 and TOP1 protein levels correlate positively with mRNA levels and furthermore that TDP1 protein level correlates positively with TDP1 catalytic activity. These positive and significant correlations suggest that both protein (e.g., IHC) and mRNA (e.g., microarray analysis) levels for TDP1 and TOP1 may be assessed during patient tumor characterization in a clinical setting.

A prevailing challenge in the clinical use of irinotecan is that some patients do not respond to treatment. Although TOP1 levels are generally thought to mediate the response to TOP1-targeting therapies, results from basal tumor TOP1 levels in clinical trial cohorts of patients treated with irinotecan regimens have been contradictory (reviewed in ref. 39). High TOP1 levels in colorectal cancer have been shown to correlate with increased irinotecan sensitivity and also sensitivity to irinotecan-containing chemoradiotherapy (9), although a subsequent study by the Dutch Colorectal Cancer Group found no correlation between TOP1 expression and response to irinotecan/5-fluorouracil chemotherapy in 545 patients (38). Identifying additional biomarkers for response may help us to better stratify patients for irinotecan treatment, selecting only those that are likely to respond. Because our TDP1 modulation studies show that TDP1 can significantly alter irinotecan sensitivity in colorectal cancer cell lines in a TOP1-dependent manner, we questioned whether TDP1 levels correlate with irinotecan response in the clinical samples. We observed no correlation between the levels of basal TOP1, TDP1, or TDP1 levels normalized to TOP1 levels, and the response to irinotecan in our panel of colorectal cancer cell lines. We also show that TDP1 expression alone as measured by IHC did not correlate with response to chemoradiotherapy with irinotecan in locally advanced rectal cancer. There may be a number of explanations for these observations. As basal TOP1 levels have been reported to affect subsequent responses (9), it is likely that the contribution of TDP1 additionally depends on TOP1 expression. Notably, removal of the apparent outlier cell line SW48 led to a positive correlation, as would be expected if TDP1 and TOP1 were dominant determinants for irinotecan sensitivity. Although the sample size was small and correlation was not significant, work is ongoing on clinical samples to further elucidate any such relationship. Specifically, future work on this cohort of patients (from the RICE trial) will additionally characterize TOP1 expression and allow for assessment of TDP1:TOP1 ratios. The response in this clinical setting is also a measure of response to irinotecan, capecitabine, and radiotherapy, not irinotecan alone. It is worth noting that a role for TDP1 in the response to IR has been previously shown in cultured cells and in mouse models (28–31, 37, 40), and will be the subject of further investigation in a clinical setting. The lack of direct correlation between TDP1 levels alone and irinotecan response is in agreement with our recent study in small cell lung cancer (41), and does not indicate that TDP1 plays a minimal role in this process. Multiple studies have shown that TOP1–DNA breaks are additionally repaired by both redundant and partially overlapping pathways driven by factors such as TDP2, Mus81, XPF-ERCC1, CtIP, and MRE11 (24, 42–46). Furthermore, the repair rate of DNA DSBs that form as a result of unrepaired TOP1–DNA SSBs may further influence irinotecan response.

In summary, our findings establish TDP1 as a potential therapeutic target for the treatment of colorectal cancer and question the validity of TOP1 or TDP1 on their own as predictive biomarkers for irinotecan response.

Disclosure of Potential Conflicts of Interest

No potential conflicts of interest were disclosed.

Authors' Contributions

Conception and design: C. Meisenberg, D.C. Gilbert, A. Chalmers, S. Gollins, S.E. Ward, S.F. El-Khamisy

Development of methodology: C. Meisenberg, D.C. Gilbert, A. Chalmers, V. Haley, S. Gollins, S.F. El-Khamisy

Acquisition of data (provided animals, acquired and managed patients, provided facilities, etc.): C. Meisenberg, D.C. Gilbert, A. Chalmers, V. Haley, S. Gollins, S.E. Ward, S.F. El-Khamisy

Analysis and interpretation of data (e.g., statistical analysis, biostatistics, computational analysis): C. Meisenberg, V. Haley, S.F. El-Khamisy

Writing, review, and/or revision of the manuscript: C. Meisenberg, D.C. Gilbert, A. Chalmers, S. Gollins, S.F. El-Khamisy

Administrative, technical, or material support (i.e., reporting or organizing data, constructing databases): C. Meisenberg, S. Gollins

Study supervision: S. Gollins, S.F. El-Khamisy

Other (devised and coordinated the study and wrote the article): S.F. El-Khamisy

Acknowledgments

The authors thank Drs. Andrew Rainey and Michael Koenig for assistance with IHC.

Grant Support

This work is funded by a Cancer Research UK grant to S.F. El-Khamisy and S.E. Ward, and by a Cancer Fund of Brighton and Sussex University Hospitals NHS Trust to D.C. Gilbert. S.F. El-Khamisy laboratory is additionally funded by a Wellcome Trust Investigator Award (103844) and a Lister Institute of Preventative Medicine Fellowship.

The costs of publication of this article were defrayed in part by the payment of page charges. This article must therefore be hereby marked *advertisement* in accordance with 18 U.S.C. Section 1734 solely to indicate this fact.

Received September 5, 2014; revised December 1, 2014; accepted December 2, 2014; published OnlineFirst December 18, 2014.

References

1. Ferlay J, Soerjomataram I, Ervik M, Dikshit R, Eser S, Mathers C, et al. Cancer incidence and mortality worldwide; 2013. Lyon, France: IARC.
2. Seymour MT, Maughan TS, Ledermann JA, Topham C, James R, Gwyther SJ, et al. Different strategies of sequential and combination chemotherapy for patients with poor prognosis advanced colorectal cancer (MRC FOCUS): a randomised controlled trial. Lancet 2007;370:143–52.
3. Saltz LB, Cox JV, Blanke C, Rosen LS, Fehrenbacher L, Moore MJ, et al. Irinotecan plus fluorouracil and leucovorin for metastatic colorectal cancer. Irinotecan Study Group. N Engl J Med 2000;343:905–14.
4. Douillard JY, Cunningham D, Roth AD, Navarro M, James RD, Karasek P, et al. Irinotecan combined with fluorouracil compared with fluorouracil alone as first-line treatment for metastatic colorectal cancer: a multicentre randomised trial. Lancet 2000;355:1041–7.
5. Gollins SS, Myint AAS, Haylock BB, Wise MM, Saunders MM, Neupane RR, et al. Preoperative chemoradiotherapy using concurrent capecitabine and irinotecan in magnetic resonance imaging-defined locally advanced rectal cancer: impact on long-term clinical outcomes. J Clin Oncol 2011;29:1042–9.

6. Willeke F, Horisberger K, Kraus-Tiefenbacher U, Wenz F, Leitner A, Hochhaus A, et al. A phase II study of capecitabine and irinotecan in combination with concurrent pelvic radiotherapy (CapIri-RT) as neoadjuvant treatment of locally advanced rectal cancer. Br J Cancer 2007;96:912–7.
7. Glynne-Jones R, Falk S, Maughan TS, Meadows HM, Sebag-Montefiore D. A phase I/II study of irinotecan when added to 5-fluorouracil and leucovorin and pelvic radiation in locally advanced rectal cancer: a Colorectal Clinical Oncology Group Study. Br J Cancer 2007;96:551–8.
8. Dopeso H, Mateo-Lozano S, Elez E, Landolfi S, Ramos Pascual FJ, Hernandez-Losa J, et al. Aprataxin tumor levels predict response of colorectal cancer patients to irinotecan-based treatment. Clin Cancer Res 2010;16:2375–82.
9. Horisberger K, Erben P, Muessle B, Woernle C, Stroebel P, Kaehler G, et al. Topoisomerase I expression correlates to response to neoadjuvant irinotecan-based chemoradiation in rectal cancer. Anticancer Drugs 2009;20:519–24.
10. Znojek P, Willmore E, Curtin NJ. Preferential potentiation of topoisomerase I poison cytotoxicity by PARP inhibition in S phase. Br J Cancer 2014;111:1319–26.
11. Carroll J, Page TKW, Chiang S-C, Kalmar B, Bode D, Greensmith L, et al. Expression of a pathogenic mutation of SOD1 sensitizes aprataxin-deficient cells and mice to oxidative stress and triggers hallmarks of premature ageing. Hum Mol Genet 2014:ddu500.
12. Wang JC. Interaction between DNA and an *Escherichia coli* protein omega. J Mol Biol 1971;55:523–33.
13. Wang JC. DNA topoisomerases. Annu Rev Biochem 1996;65:635–92.
14. Stewart L, Redinbo MR, Qiu X, Hol WG, Champoux JJ. A model for the mechanism of human topoisomerase I. Science 1998;279:1534–41.
15. Pommier Y, Pourquier P, Fan Y, Strumberg D. Mechanism of action of eukaryotic DNA topoisomerase I and drugs targeted to the enzyme. Biochim Biophys Acta 1998;1400:83–105.
16. Ashour ME, Atteya R, El-Khamisy SF. Topoisomerase mediated chromosomal break repair: emerging player in many games. Nat Rev Cancer. In press, 2015.
17. Strumberg D, Pilon AA, Smith M, Hickey R, Malkas L, Pommier Y. Conversion of topoisomerase I cleavage complexes on the leading strand of ribosomal DNA into 5′-phosphorylated DNA double-strand breaks by replication runoff. Mol Cell Biol 2000;20:3977–87.
18. Sordet O, Nakamura AJ, Redon CE, Pommier Y. DNA double-strand breaks and ATM activation by transcription-blocking DNA lesions. Cell Cycle 2010;9:274–8.
19. El-Khamisy SF, Saifi GM, Weinfeld M, Johansson F, Helleday T, Lupski JR, et al. Defective DNA single-strand break repair in spinocerebellar ataxia with axonal neuropathy-1. Nature 2005;434:108–13.
20. Interthal H, Chen HJ, Kehl-Fie TE, Zotzmann J, Leppard JB, Champoux JJ. SCAN1 mutant Tdp1 accumulates the enzyme–DNA intermediate and causes camptothecin hypersensitivity. EMBO J 2005;24:2224–33.
21. Alagoz M, Chiang S-C, Sharma A, El-Khamisy SF. ATM deficiency results in accumulation of DNA-topoisomerase I covalent intermediates in neural cells. PLoS ONE 2013;8:e58239.
22. Miao ZH, Agama K, Sordet O, Povirk L, Kohn KW, Pommier Y. Hereditary ataxia SCAN1 cells are defective for the repair of transcription-dependent topoisomerase I cleavage complexes. DNA Repair (Amst) 2006;5:1489–94.
23. Lebedeva NA, Rechkunova NI, El-Khamisy SF, Lavrik OI. Tyrosyl-DNA phosphodiesterase 1 initiates repair of apurinic/apyrimidinic sites. Biochimie 2012;94:1749–53.
24. Alagoz M, Wells OS, El-Khamisy SF. TDP1 deficiency sensitizes human cells to base damage via distinct topoisomerase I and PARP mechanisms with potential applications for cancer therapy. Nucleic Acids Res 2014;42:3089–103.
25. Hudson JJR, Chiang S-C, Wells OS, Rookyard C, El-Khamisy SF. SUMO modification of the neuroprotective protein TDP1 facilitates chromosomal single-strand break repair. Nat Commun 2012;3:733–13.
26. Katyal S, El-Khamisy SF, Russell HR, Li Y, Ju L, Caldecott KW, et al. TDP1 facilitates chromosomal single-strand break repair in neurons and is neuroprotective *in vivo*. EMBO J. 2007;26:4720–31.
27. Barthelmes HU, Habermeyer M, Christensen MO, Mielke C, Interthal H, Pouliot JJ, et al. TDP1 overexpression in human cells counteracts DNA damage mediated by topoisomerases I and II. J Biol Chem 2004;279:55618–25.
28. Chiang S-C, Carroll J, El-Khamisy SF. TDP1 serine 81 promotes interaction with DNA ligase IIIalpha and facilitates cell survival following DNA damage. Cell Cycle 2010;9:588–95.
29. El-Khamisy SF, Hartsuiker E, Caldecott KW. TDP1 facilitates repair of ionizing radiation-induced DNA single-strand breaks. DNA Repair (Amst) 2007;6:1485–95.
30. Zhou T, Lee JW, Tatavarthi H, Lupski JR, Valerie K, Povirk LF. Deficiency in 3′-phosphoglycolate processing in human cells with a hereditary mutation in tyrosyl-DNA phosphodiesterase (TDP1). Nucleic Acids Res 2005;33:289–97.
31. Zhou T, Akopiants K, Mohapatra S, Lin PS, Valerie K, Ramsden DA, et al. Tyrosyl-DNA phosphodiesterase and the repair of 3′-phosphoglycolate-terminated DNA double-strand breaks. DNA Repair (Amst) 2009;8:901–11.
32. Alagoz M, Gilbert DC, El-Khamisy S, Chalmers AJ. DNA repair and resistance to topoisomerase I inhibitors: mechanisms, biomarkers and therapeutic targets. Curr Med Chem 2012;19:3874–85.
33. Walker S, Meisenberg C, Bibby RA, Askwith T, Williams G, Rininsland FH, et al. Development of an oligonucleotide-based fluorescence assay for the identification of tyrosyl-DNA phosphodiesterase 1 (TDP1) inhibitors. Anal Biochem 2014;454:17–22.
34. Marchand C, Lea WA, Jadhav A, Dexheimer TS, Austin CP, Inglese J, et al. Identification of phosphotyrosine mimetic inhibitors of human tyrosyl-DNA phosphodiesterase I by a novel AlphaScreen high-throughput assay. Mol Cancer Ther 2009;8:240–8.
35. Weidlich IE, Dexheimer T, Marchand C, Antony S, Pommier Y, Nicklaus MC. Inhibitors of human tyrosyl-DNA phospodiesterase (hTdp1) developed by virtual screening using ligand-based pharmacophores. Bioorg Med Chem 2010;18:182–9.
36. Breslin C, Clements PM, El-Khamisy SF, Petermann E, Iles N, Caldecott KW. Measurement of chromosomal DNA single-strand breaks and replication fork progression rates. Meth Enzymol 2006;409:410–25.
37. El-Khamisy SF. To live or to die: a matter of processing damaged DNA termini in neurons. EMBO Mol Med 2011;3:78–88.
38. Koopman M, Venderbosch S, van Tinteren H, Ligtenberg MJ, Nagtegaal I, Van Krieken JH, et al. Predictive and prognostic markers for the outcome of chemotherapy in advanced colorectal cancer, a retrospective analysis of the phase III randomised CAIRO study. Eur J Cancer 2009;45:1999–2006.
39. Gilbert DC, Chalmers AJ, El-Khamisy SF. Topoisomerase I inhibition in colorectal cancer: biomarkers and therapeutic targets. Br J Cancer 2011;106:18–24.
40. El-Khamisy SF, Katyal S, Patel P, Ju L, McKinnon PJ, Caldecott KW. Synergistic decrease of DNA single-strand break repair rates in mouse neural cells lacking both Tdp1 and aprataxin. DNA Repair (Amst) 2009;8:760–6.
41. Meisenberg C, Ward SE, Schmid P, El-Khamisy SF. TDP1/TOP1 ratio as a promising indicator for the response of small cell lung cancer to topotecan. J Cancer Sci Ther 2014;6:258–67.
42. Zeng Z, Sharma A, Ju L, Murai J, Umans L, Vermeire L, et al. TDP2 promotes repair of topoisomerase I-mediated DNA damage in the absence of TDP1. Nucleic Acids Res 2012;40:8371–80.
43. Hamilton NK, Maizels N. MRE11 function in response to topoisomerase poisons is independent of its function in double-strand break repair in saccharomyces cerevisiae. PLoS ONE 2010;5:e15387.
44. Zhang YW, Regairaz M, Seiler JA, Agama KK, Doroshow JH, Pommier Y. Poly(ADP-ribose) polymerase and XPF-ERCC1 participate in distinct pathways for the repair of topoisomerase I-induced DNA damage in mammalian cells. Nucleic Acids Res 2011;39:3607–20.
45. Regairaz M, Zhang Y-W, Fu H, Agama KK, Tata N, Agrawal S, et al. Mus81-mediated DNA cleavage resolves replication forks stalled by topoisomerase I-DNA complexes. J Cell Biol 2011;195:739–49.
46. Hartsuiker E, Mizuno K, Molnar M, Kohli J, Ohta K, Carr AM. Ctp1CtIP and Rad32Mre11 nuclease activity are required for Rec12Spo11 removal, but Rec12Spo11 removal is dispensable for other MRN-dependent meiotic functions. Mol Cell Biol 2009;29:1671–81.

Published OnlineFirst December 18, 2014; DOI: 10.1158/1535-7163.MCT-14-0762

Molecular Cancer Therapeutics

Clinical and Cellular Roles for TDP1 and TOP1 in Modulating Colorectal Cancer Response to Irinotecan

Cornelia Meisenberg, Duncan C. Gilbert, Anthony Chalmers, et al.

Mol Cancer Ther 2015;14:575-585. Published OnlineFirst December 18, 2014.